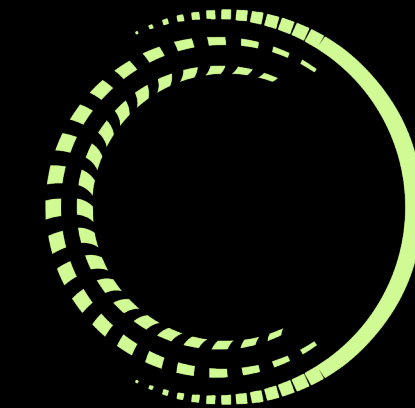


THEA ENERGY [Thu-Mo-Po.09-02] Instrumentation of the Canis 3x3 superconducting magnet array

M. Dickerson, A. Doudna Cate, B. Chen, C.Khurana, D. Nash, A. Saucedo, M. Savastianov, M. Slepchenkov, and S. Srinivasan



Introduction

This poster addresses the topics of instrumentation configuration of Thea Energy, Inc.'s "Canis" 3x3 array of high-temperature superconductor (HTS) planar coil magnets [1], highlighting magnet modularity and the field validation support system. This poster explores the two schemes for the planar coil magnet instrumentation configurations along with sensor count, position, and routing. Measurement error relative to simulation error I also discussed in the context of magnetic field shape produced by the array. These techniques culminate in the verification of the Stellarator relevant field shapes produced by the magnet array.

Modular Magnet Instrumentation

The Canis planar coil magnets were designed for ease of removal and high configurability.

- Limited number of instrumentation feedthroughs restricted the total number connections
- Number of voltage taps and temperature sensors mounted on winding packs varied for optimal use of available feedthroughs
- Designation of resolution scheme was based primary on whether a winding pack would see distinctive magnetic field contours or if the winding pack was in a quenching location
- Previous characterization of the winding pack played a minor role in winding pack resolution schema determination

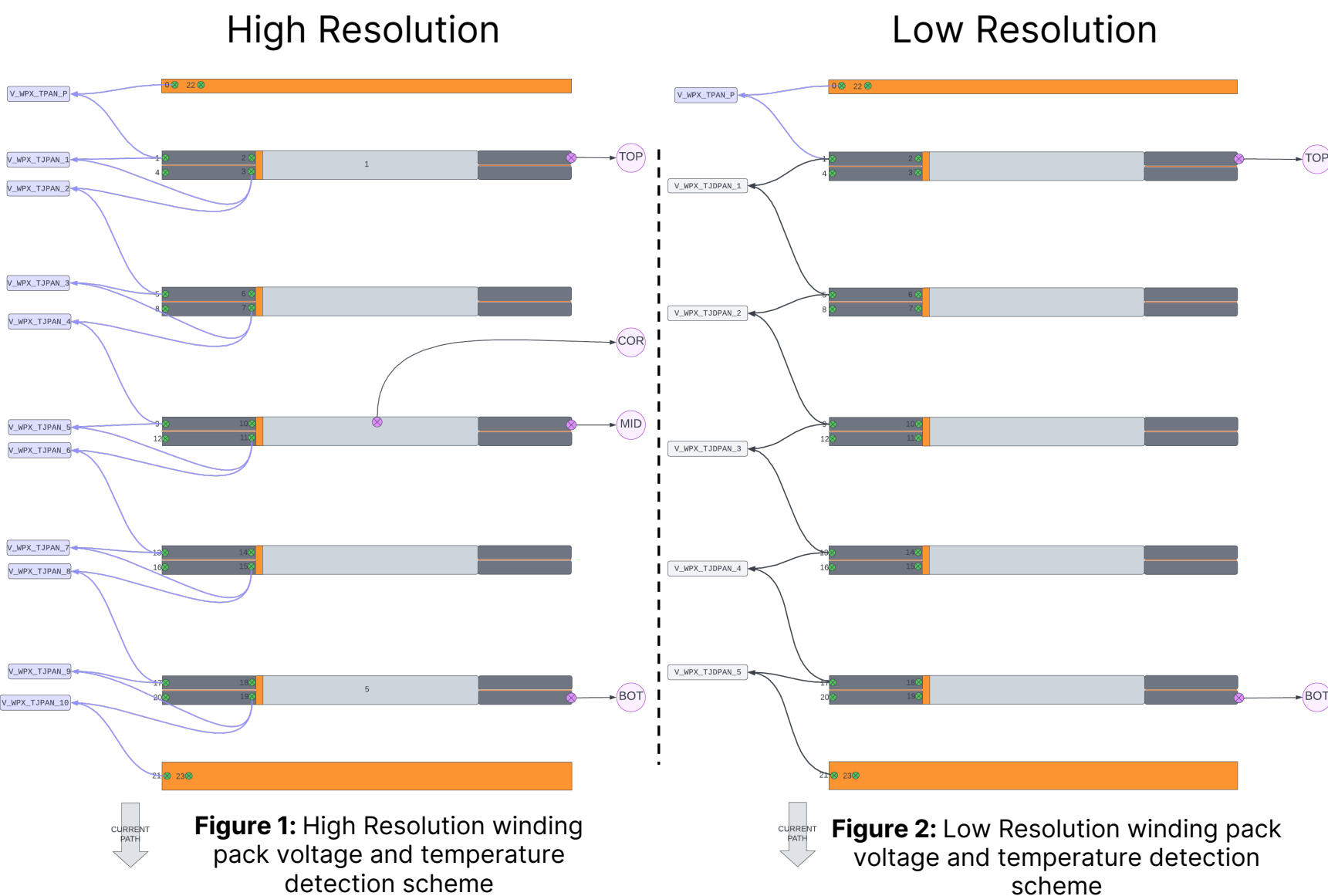


Figure 1: High Resolution winding pack voltage and temperature detection scheme

Figure 2: Low Resolution winding pack voltage and temperature detection scheme



Figure 3: Canis 3x3 array with mounted Winding Pack Instrumentation Board

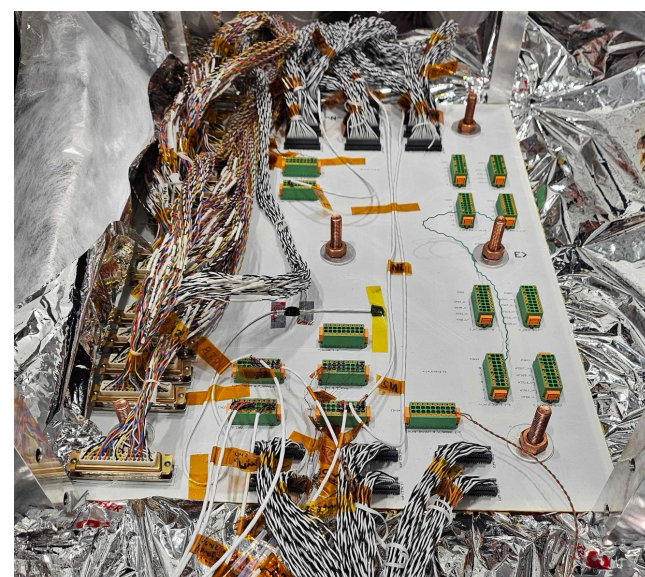


Figure 4: Connections being routed to the Canis Instrumentation Board in its final position

All winding packs shared the same harnessing methods, show above, and connected to a large instrumentation board.

- A PCB was fastened to a structural plate on top of the winding pack
- All magnet voltage taps and temperature detectors, along with Hall effect probe routed to this board
- Signals were paired and sent out to a larger Canis Instrumentation Board (CIB) which removed any extraneous signals
- Sensors monitoring ScHe flow, structural temperature, and input leads temperature and voltage were connected to the CIB
- CIB was conductively cooled to 80°K via internal 1oz copper plane, acting as a thermal anchor for instrumentation wires by dissipating the heat load from the 293°K to 80°K transition

Total Connections in the Canis 3x3 Array			
Type	Winding Packs	Cryo-Vessel	Total Wires
Twisted Pairs	137	27	328
Cernoxes	26	22	192
PT100	0	24	96
Hall Effect	9	0	36
ScHe Flow	0	2	4
Spares	18	4	44
Total	190	79	700

Table 1: Total instrumentation connections located on the Canis Instrumentation Board

Magnetic Field Measurement

To demonstrate that the Canis 3x3 array could create stellarator relevant field shapes, the magnetic field accuracy needed to be validated.

- Root Mean Square Error was calculated using the simulated magnetic field compared to measured, then normalized to the maximum field seen.
- Magnetic field Root Mean Squared Error was to be less than 1%.
- A gantry that scanned magnetic field in a square 1.6m² plane with grid spacing of 12mm was placed external to the vacuum vessel.
- The gantry used Metrolab 3-axis THM1176-MF calibrated with an accuracy of ±0.1% along each axis and resolution 0.1mT.

$$E_{RMS} = \frac{\sqrt{\frac{1}{N} \sum_{i=1}^N (B_{z,meas,i} - B_{z,pred,i})^2}}{|B_{z,pred,max}|}$$

Equation 1: Normalized root mean squared error for measured versus predicted z-axis magnetic field

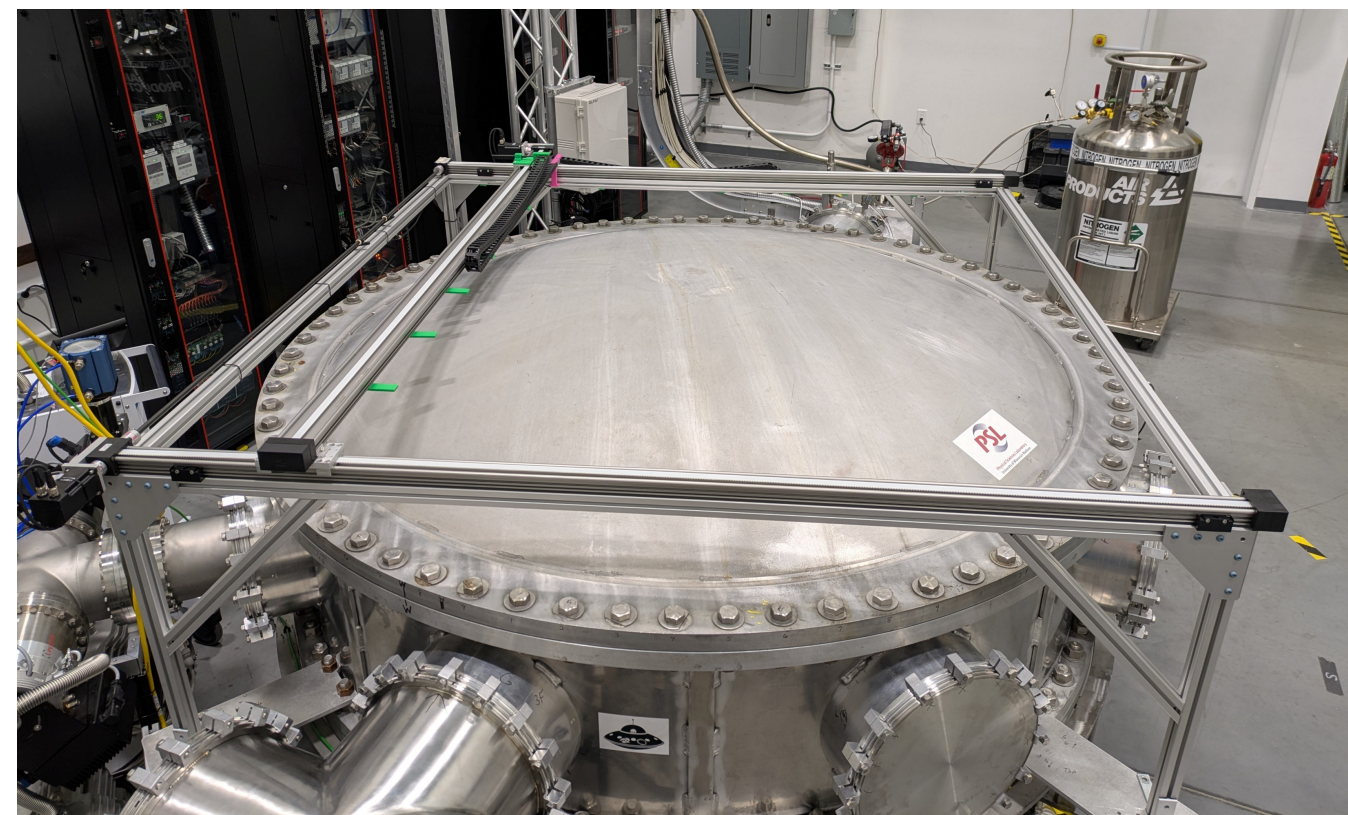


Figure 5: Magnetic field scanning gantry (Atlas) placed on top the vacuum vessel.

A thorough consideration of magnetic field error sources was coupled with an optimization of the external field probe's Degrees of Freedom to meet the ERMS requirements.

- The Canis 3x3 array was energized to a contrasting "checkboard" pattern that provided the greatest contrast in winding pack locations
- A Nelder-Mean optimization was used to approximate the coordinate offsets of the gantry field probe scan [2]
 - 3 DOF for the XYZ position of the scan plane relative to the magnet array
 - 3 DOF for the angular rotation of the scan plane about the array XYZ axes
 - 3 DOF for the angular orientation of the probe with respect to the gantry
- The root mean square error was then bounded by a Monte-Carlo simulation of 7,578 perturbations
- The 95th percentile of the calculated ERMS was 0.91% and 0.94% for the two field shapes tested



Figure 6: "Checkboard" magnet array excitation pattern, red indicated positive current flow black indicates negative current flow while HIGH/LOW designates magnet resolution

Atlas Orientation for Field Error Estimation			
Group	Degrees of Freedoms		
	X	Y	Z
Scan Plane Offset [m]	-0.9508	-0.9362	0.2418
Scan Plane Rotation [°]	-0.0262	0.0254	72.70
Hall Probe Rotation [°]	-0.484	-0.808	0.330

Table 2: Degrees of freedom estimation based on Nelder-Mead optimization

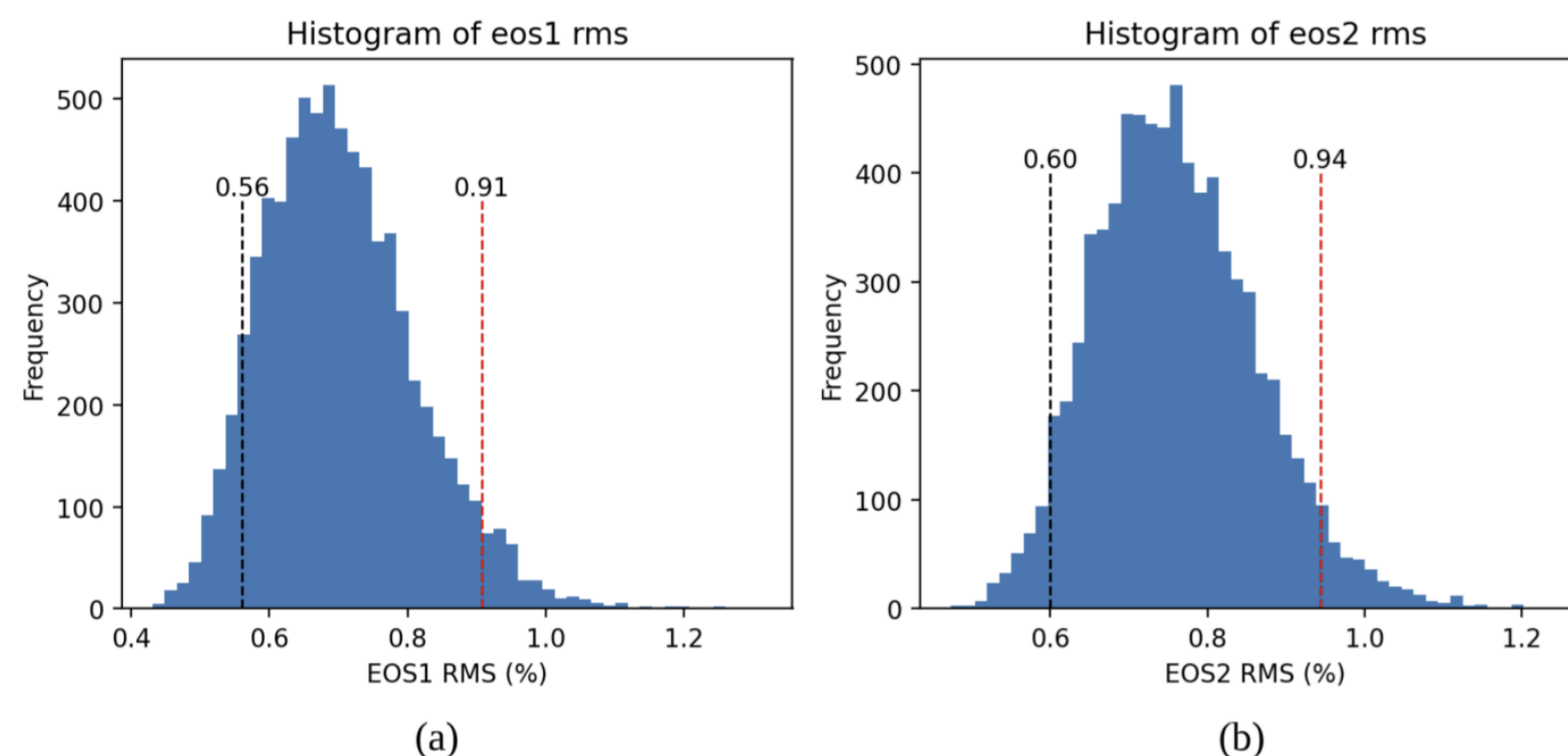


Figure 7: Histogram of resulting ERMS values for (a) EOS1 relevant field shape and (b) EOS2 relevant field shape

Conclusion

This poster emphasized the instrumentation modularity and magnetic field validation methods implemented in the Canis 3x3 array. Two distinct resolution schemas with varying sensor counts were developed based on magnet placement in array. Through optimization of an external magnetic field scanning system's degrees of freedom, the created magnetic field shape was validated. The instrumentation architecture presented in this poster effectively verified that the RMS field error produced by the magnet array was less than 1%, thus proving the Stellarator relevant field shaping of the Canis project.

Acknowledgements and References

- "Planar coil stellarator," Patent PCT/US2023/063 949, March 8, 2023, published as WO/2023/178004, US Patent 12,100,520.
- Nash, D., et al. (2025). Prototyping and Test of the "Canis" HTS Planar Coil Array for Stellarator Field Shaping ArXiv. <https://doi.org/2503.18960>

